Curvature Effect on Compressible Turbulent Flow over a Wavy Wall *

SUN Xiao-Bo(孙小波), LU Xi-Yun(陆夕云)**

Department of Modern Mechanics, University of Science and Technology of China, Hefei 230027

(Received 16 May 2007)

A fully developed compressible turbulent flow in a channel with a lower wavy wall and a upper plane wall is studied using large eddy simulation. We mainly attempt to deal with the curvature effect on compressible turbulent flow over the wavy wall. Some typical quantities including the mean turbulence statistics, dilatation and baroclinic terms in the enstrophy equation, turbulent kinetic energy budgets and the near-wall turbulent structures are analysed. The results obtained in this study provide physical insight into the understanding of the effects of curvature and compressibility on wall-bounded compressible turbulent flow.

PACS: 47.27.−e, 47.27.Ep

It is important to understand the mechanisms of wall-bounded compressible flow in fundamentals and applications. Usually, a fully developed compressible turbulent channel flow is used as a typical model problem and has been extensively studied using direct numerical simulation (DNS) or large eddy simulation (LES). Coleman *et al.*[1] and Huang *et al.*[2] performed DNS studies of turbulent supersonic flow in an isothermal-wall plane channel and investigated some typical issues in modeling compressible shear flows. Morinishi *et al.*[3] carried out a DNS to deal with the effects of isothermal- and adiabatic-wall conditions on the compressible turbulent channel flow. Lenormand *et al.*[4] performed an LES of subsonic and supersonic channel flow to examine the subgrid-scale (SGS) models of compressible turbulent flow. These investigations were mainly focused on the similarity and difference between compressible and incompressible wall-bounded turbulent flows based on the Van Driest density-weighted transformation.

Following some typical studies of incompressible flow over a wavy wall,[5,6] it is found that the wall curvature has a significant influence on flow behaviour. The relevant work also exhibited that the wall shape has a great effect on compressible turbulent flow.[7,8] To our knowledge, however, the curvature effect on compressible turbulent flow has never been studied and is highly desired to understand the coupled influence of curvature and compressibility on compressible turbulent flow.

A configuration used here is a channel with a lower wavy wall and a upper plane wall. The wavy wall is given by $h_w = a\cos(2\pi x/\lambda)$ with a the amplitude and λ the wave length. The no-slip and isothermal boundary conditions are exerted on both the walls. Periodic boundary conditions are used in the streamwise and spanwise direction. The relevant parameters are described as follows. The Reynolds number is defined as $\mathrm{Re} = \rho_m U_m \lambda/\mu_w$ with ρ_m the bulk density, U_m the bulk velocity and μ_w the viscosity at the isothermal wall. The Mach number based on the sound speed at the isothermal wall is $M = U_m/(\gamma R T_w)^{1/2}$ with $R = (\gamma - 1)C_p/\gamma$ the gas constant. The viscosity is given by Sutherland's law, i.e., $\mu = T^{3/2}(1 + S_1/T_w)/(T + S_1/T_w)$, where $S_1 = 110.4\,\mathrm{K}$ and $T_w = 293.15\,\mathrm{K}$. The parameters in the present calculations are $\mathrm{Re} = 3000\pi$, $M = 0.5$, $\mathrm{Pr} = 0.7$, and $\gamma = 1.4$. The amplitude relative to the wave length is chosen as $a = 0.01$, 0.02 and 0.03, respectively.

Here, an LES approach of compressible turbulent flow without density weighting (or Favre averaging) is used. Thus, the resolved quantities can be really obtained using this novel LES approach.[9] The governing equations and numerical methods have been described in Ref. [9]. Based on the selection of computational parameters for compressible turbulent channel flows,[1−4] the computational domain is chosen as $[0, 4\lambda] \times [0, 3\lambda/2] \times [0, 2\lambda/\pi]$ with the grid number 160, 80 and 192 in the streamwise, spanwise and vertical direction, denoted by $x_1(x)$, $x_2(y)$ and $x_3(z)$, respectively; the corresponding velocity components represent $u_1(u)$, $u_2(v)$ and $u_3(w)$. To ensure the computational domain size to be enough, the two-point correlations of the fluctuations for typical variables in the x- and y-directions are calculated to be negligibly small. The grids are uniform in the y-direction and stretching distribution in the x- and z-directions. The nearest wall grid spacing expressed in wall units is $\triangle z^+ \approx 0.8$ for both the walls. Based on our extensive test and previous validation,[9] the code and computational parameters used can reliably predict the turbulent flow characteristics.

To deal with the curvature effect on compressible turbulent flow, typical results near the wavy wall are mainly analysed. Figure 1 shows the mean stream-

* Supported by the National Natural Science Foundation of China under Grant Nos 90405007 and 10125210, and the Programme for Changjiang Scholars and Innovative Research Team in the University.

** To whom correspondence should be addressed. Email: xlu@ustc.edu.cn

wise velocity and turbulence intensities at $x/\lambda = 0$ (crest) and 0.5 (trough), where the mean or Reynolds average quantities are denoted by $\langle\ \rangle$ and obtained by taking time- and space-average in the spanwise direction and then phase-average over four wavelengths in the streamwise direction. As shown in Figs. 1(a) and 1(b) for the mean velocity $\langle u \rangle$, the fluid moves rapidly over the crest and the mean velocity increases with the amplitude in the core region of the channel. Since small-amplitude waves and subsonic flow are considered here, no separation and shocklet are identified. Further, to exhibit the curvature effect on compressibility based on the mean quantities, Fig. 2(a) typically shows the contours of the mean dilatation $\langle \partial u_i/\partial x_i \rangle$ at $a = 0.03$. It is reasonably predicted that compressed flow with negative dilatation occurs over the crest region and expanded flow with positive dilatation over the trough region. The locations of the maximum compression and expansion are around $x/\lambda = 0.05$ and 0.4, respectively. Based on our calculated results, as the amplitude increases, the extremum of $\langle \partial u_i/\partial x_i \rangle$ is strengthened, and its location is nearly unchanged in the streamwise direction and leaves further away from the wavy wall in the vertical direction. Compared with the dilatation distribution for a turbulent supersonic plane channel flow,[1] it is found that the curvature effect has significantly strengthened the mean dilatation.

As shown in Figs. 1(c)–1(h), the turbulence intensities (i.e., u'^{+}_{rms}, v'^{+}_{rms} and w'^{+}_{rms}) increase with the amplitude. It is noticed that the streamwise intensity near the wall is enhanced over the crest in Fig. 1(c)

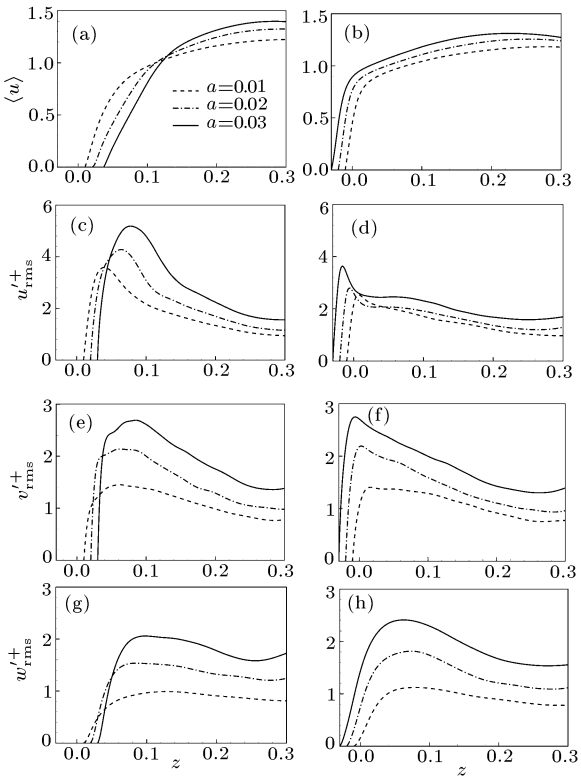

Fig. 1. Mean streamwise velocity and turbulence intensities at the crest $x/\lambda = 0$ (left column) and trough $x/\lambda = 0.5$ (right column): (a) and (b) streamwise velocity $\langle u \rangle$; (c) and (d) streamwise intensity u'^{+}_{rms}; (e) and (f) spanwise intensity v'^{+}_{rms}; (g) and (h) vertical intensity w'^{+}_{rms}, where + denotes the quantities normalized by u_τ with $a = 0$. Here *rms* means the root-mean-square value of fluctuation.

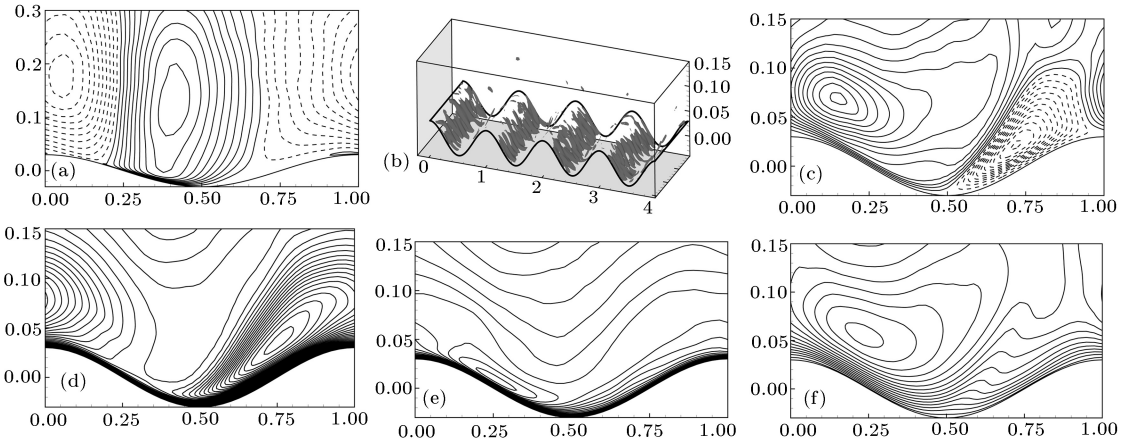

Fig. 2. Flow structures at $a = 0.03$: (a) mean dilatation $\langle \partial u_i/\partial x_i \rangle$ with contour increment 0.1; (b) isosurface of instantaneous enstrophy $\omega_i\omega_i/2$; (c) Reynolds shear stress $-(u'w')^{+}$ with increment 0.2; (d) u'^{+}_{rms} with increment 0.2; (e) v'^{+}_{rms} with increment 0.2; (f) w'^{+}_{rms} with increment 0.2. Here, the solid lines represent positive values and the dashed lines the negative values.

and suppressed over the trough in Fig. 1(d). Correspondingly, the spanwise intensity is strengthened over the trough in Fig. 1(f). Similar behaviour was also found for incompressible turbulent flow over a wavy wall.[5] They argued that it may be associated with temporally persistent vortex-like structures localized near the surface. To demonstrate the vortical structures near the wall, the instantaneous enstrophy (i.e., $\omega_i\omega_i/2$) over the wavy wall at $a = 0.03$ is shown in Fig. 2(b). It is seen that the well-organized stream-

wise vortical structures, corresponding to the high- and low-speed steaks based on the streamwise velocity fluctuation, occur over the downslope surface. As indicated by Henn and Sykes,[5] these vortical structures are relevant to the turbulent kinetic energy transfer between the streamwise and other directions.

To exhibit a global view of the turbulence statistics over the wavy wall, the contours of the Reynolds shear stress and turbulence intensities are shown in Figs. 2(c)–2(f) for $a = 0.03$. The Reynolds shear stress $-(u'w')^+$ shows the positive and negative extrema localized around $x/\lambda = 0.15$ and 0.75 in Fig. 2(c), respectively. The distribution of the Reynolds stress is closely associated with that of the streamwise velocity fluctuation in Fig. 2(d). The streamwise intensity is strengthened over the upslope surface. The relatively strong spanwise and vertical intensities occur over the downslope surface. We also identify that the streamwise intensity contributes a major part to turbulent kinetic energy with a similar pattern shown in Fig. 2(d). In addition, we have examined the contours of the density and temperature fluctuations over the wavy wall and found that their maxima locate over the upslope surface, consistent with the streamwise velocity fluctuation.

Vorticity dynamics are closely associated with turbulence characteristics.[10−12] To understand the influence of typical effects (e.g., dilatation and baroclinic effect) on the compressible flow, we analyse some terms in the enstrophy transport equation, which is described as

$$\frac{d}{dt}\left(\frac{1}{2}|\boldsymbol{\omega}|^2\right) = \boldsymbol{\omega}\cdot\boldsymbol{S}\cdot\boldsymbol{\omega} - |\boldsymbol{\omega}|^2(\nabla\cdot\boldsymbol{u}) + \frac{\nabla\rho\times\nabla p}{\rho^2}\cdot\boldsymbol{\omega} + VT, \tag{1}$$

where $\boldsymbol{u}$ and $\boldsymbol{\omega}$ represent the velocity and vorticity vector, respectively, $\boldsymbol{S}$ is the strain tensor, and VT denotes the viscous terms. The first, second and third terms on the right-hand side of Eq. (1) can be referred as the stretching, dilatation and baroclinic term,[12] respectively, and denoted by term-1, term-2 and term-3. Figure 3 shows the distributions of the mean enstrophy and three terms along the wavy wall surface and a line away from the wavy surface with $z - h_w \approx 0.004$. The high enstrophy distribution occurs along the downslope surface, consistent with the vortical structures in Fig. 2(b). The peak value of enstrophy locates at $x = 0.3$ approximately on the wavy surface in Fig. 3(a), and becomes smaller with its location (i.e., $x = 0.35$) shifting downstream on the line in Fig. 3(b). Compared with Figs. 3(a) and 3(b), it is reasonably found that the enstrophy decreases quickly with the distance away from the wall surface.

The mean stretching term (i.e., term-1) is zero on the wall surface in Fig. 3(a), in agreement with the vorticity dynamics analysis,[12] and becomes main contribution to the enstrophy in the flow field in Fig. 3(b), in particular over the downslope surface. The stretching effect may have a significant role on the turbulent energy production and transfer.[10−12] Thus, the strong stretching effect over the downslope surface is reasonably relevant to enhancing the spanwise and vertical intensities in Figs. 2(e) and 2(f). The mean dilatation term (i.e., term-2) also has an important influence on the enstrophy in the flow field, e.g., over the region of $0.25 < x < 0.5$ in Fig. 3(b). Based on the distributions of the mean vorticity magnitude and dilatation, we can find that the term-2 is mainly controlled by the vorticity magnitude square along the wall surface and by the dilatation in the flow field. The baroclinic term (i.e., term-3) exhibits a major contribution to the enstrophy along the wall surface, in particular the downslope surface, and becomes weak in the flow field.

The turbulent kinetic energy budgets for compressible flow are further analysed. To simplify the treatment of turbulent kinetic energy equation, the Favre decomposition is introduced here. The turbulent kinetic energy equation for compressible flow is given as[2]

$$\frac{\partial\langle\rho\rangle\{u_k\}\{k\}}{\partial x_k} = EP + TD + VP + VD + ED + CT_1 + CT_2 + CT_3, \tag{2}$$

where $\{k\} = \{u_i''\}^2/2$ represents the turbulent kinetic energy, $EP = -\langle\rho\rangle\{u_i''u_k''\}\partial\{u_i\}/\partial x_k$ the energy production, $TD = -\partial\langle\rho\rangle\{u_k''k''\}/\partial x_k$ the turbulent diffusion, $VP = -\partial\langle p'u_k'\rangle/\partial x_k$ the diffusion due to velocity-pressure interaction, $VD = \partial\langle\tau_{ik}'u_i'\rangle/\partial x_k$ the viscous diffusion, $ED = -\langle\tau_{ik}'\partial u_i'/\partial x_k\rangle$ the energy dissipation, and $CT_1 = -\langle u_k''\rangle\partial\langle p\rangle/\partial x_k$, $CT_2 = \langle u_i''\rangle\partial\langle\tau_{ik}\rangle/\partial x_k$, and $CT_3 = \langle p'\partial u_k'/\partial x_k\rangle$ are the compressibility-related terms. The symbol $\{\ \}$ means the Favre average, i.e., $\{f\} = \langle\rho f\rangle/\langle\rho\rangle$. The single prime $'$ and the double prime $''$ represent the turbulent fluctuations with respect to the Reynolds and Favre average, respectively.

Based on the mean kinetic energy and internal energy equations, we can identify that the terms EP, CT_1 and CT_2 in Eq. (2) are responsible for the energy exchange between the mean kinetic and turbulent kinetic energy, and the terms ED and CT_3 for the energy exchange between the internal and turbulent kinetic energy. The contours of four typical terms over the wavy wall at $a = 0.03$ are shown in Fig. 4. It is reasonably predicted that a major energy production EP occurs over the upslope surface in Fig. 4(a), consistent with the contours of turbulent kinetic energy or streamwise intensity in Fig. 2(d). Due to the curvature effect, a small negative distribution of EP appears near the wall in the region of $0 < x < 0.25$ approximately, indicating the turbulent kinetic energy transferring back to the mean flow. From the contours of the energy dissipation ED (not shown here), it is observed that the distribution is mainly limited in the viscous layer over the wavy wall with negative

value, which acts as a source term in the internal energy equation. In addition, the distributions of other terms, i.e., TD, VP and VD in Eq. (2), have similar behaviours to the incompressible turbulent flow over a wavy wall.

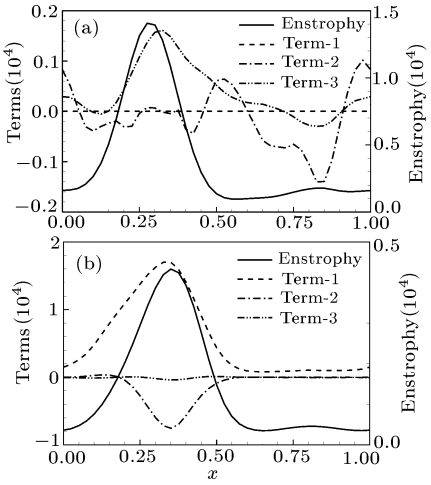

Fig. 3. Distributions of the mean enstrophy and three terms in Eq. (1) along (a) the wavy wall surface and (b) a line away from the wavy surface with $z - h_w \approx 0.004$ for $a = 0.03$.

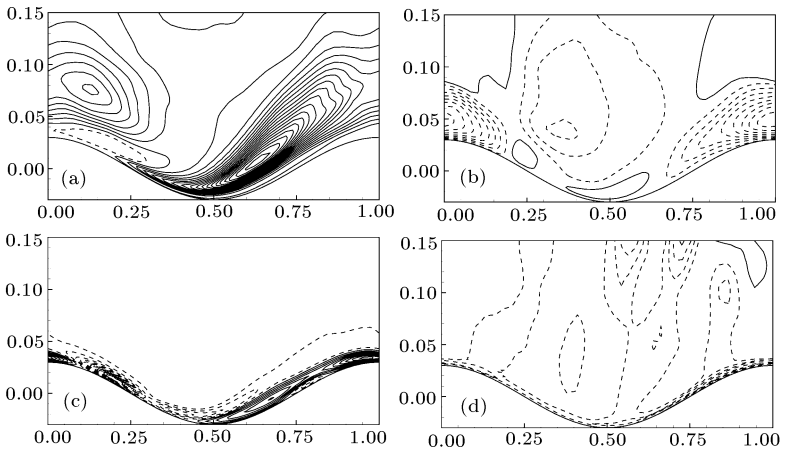

Fig. 4. Turbulent kinetic energy budgets at $a = 0.03$: (a) energy production term EP with contour increment 5; (b) velocity-pressure gradient term CT_1 with increment 0.3; (c) velocity-viscous term CT_2 with increment 0.1; (d) pressure-dilatation term CT_3 with increment 0.2. Here, solid lines represent positive values and dashed lines negative values.

Here, we are interested in the curvature effect on the compressibility-related terms. The velocity-pressure gradient term CT_1 has a notably negative contribution to the budget balance over the crest region in Fig. 4(b). The velocity-viscous term CT_2 shows an obvious variation in the viscous layer in Fig. 4(c). The term CT_2 takes a negative contribution to the budget balance over the downslope surface and a positive contribution over the upslope surface. The negative distributions of CT_1 and CT_2 over the wavy wall mean that the turbulent kinetic energy transfers back to the mean flow under the coupled influence of the compressibility and curvature effect. The distribution over the wavy wall of the pressure-dilatation term CT_3 is shown in Fig. 4(d). The influence of the term CT_3 spreads over the flow field, consistent with the mean dilatation distribution in Fig. 2(a). The negative distributions near the wall and in the flow field represent that the turbulent kinetic energy transfers to the internal energy. In addition, we have identified that the magnitudes of the compressibility-related terms exhibit the same order, unlike the major compressibility contribution only from CT_2 for compressible plane channel flow.[2] The curvature effect has significantly enhanced the compressibility-related terms, compared with the distributions of these terms over the compressible plane channel flow.[1,2]

In summary, the curvature effect on compressible turbulent flow over a wavy wall has been investigated. According to some typical quantities including the mean turbulence statistics, dilatation and baroclinic terms in the enstrophy equation, turbulent kinetic energy budgets and the near-wall turbulent structures, we have found that the curvature effect has significantly enhanced the influence of compressibility on wall-bounded turbulent flow. Although we recognize the limitation of analysis based on only typical results, the present effort has provided physical insight into the understanding of the coupled effects of curvature and compressibility on wall-bounded compressible turbulent flow.

We thank Professor P. Sagaut for providing a compressible Navier-Stokes basic code.

References

[1] Coleman G N, Kim J. and Moser R D 1995 *J. Fluid Mech.* **305** 159
[2] Huang P G, Coleman G N and Bradshaw P 1995 *J. Fluid Mech.* **305** 185
[3] Morinishi Y, Tamano S and Nakabayashi K 2004 *J. Fluid Mech.* **502** 273
[4] Lenormand E, Sagaut P, Ta Phuoc L and Comte P 2000 *AIAA J.* **38** 1340
[[5] Henn D S and Sykes R I 1999 *J. Fluid Mech.* **383** 75
[6] Dong G J and Lu X Y 2007 *Phys. Fluids* **19** 057107
[7] Adams N A 2000 *J. Fluid Mech.* **420** 47
[8] Lu X Y, Wang S W, Sung H G, Hsieh S Y and Yang V 2005 *J. Fluid Mech.* **527** 171
[9] Sun X B and Lu X Y 2006 *Phys. Fluids* **18** 118101
[10] Chorin A J 1994 *Vorticity and Turbulence* (Springer-Verlag, Berlin)
[11] Wu J Z, Zhou Y, Lu X Y and Fan M 1999 *Phys. Fluids* **11** 627
[12] Wu J Z, Ma H Y and Zhou M D 2006 *Vorticity and Vortex Dynamics* (Berlin: Springer)